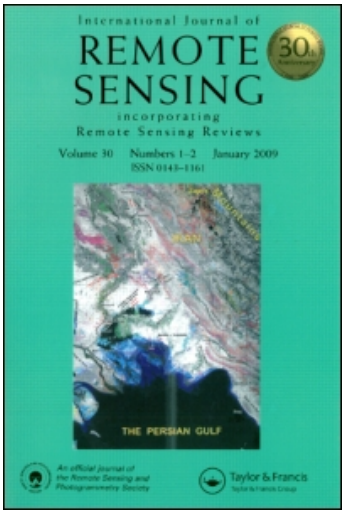

International Journal of Remote Sensing
Publication details, including instructions for authors and subscription information:
http://www.informaworld.com/smpp/title~content=t713722504

Integrating LIDAR elevation data, multi-spectral imagery and neural network modelling for marsh characterization

James T. Morris[ab]; Dwayne Porter[bc]; Matt Neet[b]; Peter A. Noble[d]; Laura Schmidt[b]; Lewis A. Lapine[e]; John R. Jensen[bf]
[a] Department of Biological Sciences, University of South Carolina, Columbia, USA [b] Belle W. Baruch Institute for Marine and Coastal Sciences, University of South Carolina, Columbia, USA [c] Department of Environmental Health Sciences, University of South Carolina, Columbia, USA [d] Department of Civil and Environmental Engineering, University of Washington, Seattle, USA [e] South Carolina Geodetic Survey, Columbia, South Carolina, USA [f] Department of Geography, University of South Carolina, Columbia, USA

To cite this Article Morris, James T. , Porter, Dwayne , Neet, Matt , Noble, Peter A. , Schmidt, Laura , Lapine, Lewis A. and Jensen, John R.(2005) 'Integrating LIDAR elevation data, multi-spectral imagery and neural network modelling for marsh characterization', International Journal of Remote Sensing, 26: 23, 5221 — 5234
To link to this Article: DOI: 10.1080/01431160500219018
URL: http://dx.doi.org/10.1080/01431160500219018

International Journal of Remote Sensing
Vol. 26, No. 23, 10 December 2005, 5221–5234

Integrating LIDAR elevation data, multi-spectral imagery and neural network modelling for marsh characterization

JAMES T. MORRIS*†‡, DWAYNE PORTER‡§, MATT NEET‡, PETER A. NOBLE¶, LAURA SCHMIDT‡, LEWIS A. LAPINE and JOHN R. JENSEN‡††

†Department of Biological Sciences, University of South Carolina, Columbia, SC 29208, USA

‡Belle W. Baruch Institute for Marine and Coastal Sciences, University of South Carolina, Columbia, SC 29208, USA

§Department of Environmental Health Sciences, University of South Carolina, Columbia, SC 29208, USA

¶Department of Civil and Environmental Engineering, University of Washington, Seattle, WA 98195, USA

**South Carolina Geodetic Survey, Columbia, South Carolina, 29210, USA

††Department of Geography, University of South Carolina, Columbia, SC 29208, USA

Vertical elevation relative to mean sea level is a critical variable for the productivity and stability of salt marshes. This research classified a high spatial resolution Airborne Data Acquisition and Registration (ADAR) digital camera image of a salt marsh landscape at North Inlet, South Carolina, USA using an artificial neural network. The remote sensing-derived thematic map was cross-referenced with Light Detection and Ranging (LIDAR) elevation data to compute the frequency distribution of marsh elevation relative to tidal elevations. At North Inlet, the median elevation of the salt marsh dominated by *Spartina alterniflora* was 0.349 m relative to the North American Vertical Datum 1988 (NAVD88), while the mean high water level was 0.618 m (2001 to May, 2003) with a mean tidal range of 1.39 m. The distribution of elevations of *Spartina* habitat within its vertical range was normal, and 80% of the salt marsh was situated between a narrow range of 0.22 m and 0.481 m. Areas classified as *Juncus* marsh, dominated by *Juncus roemerianus*, had a broader, skewed distribution, with 80% of the distribution between 0.296 m and 0.981 m and a median elevation of 0.519 m. The *Juncus* marsh occurs within the intertidal region of brackish marshes and along the upper fringe of salt marshes. The relative elevation of the *Spartina* marsh at North Inlet is consistent with recent work that predicts a decrease in equilibrium elevation with an increasing rate of sea-level rise and suggests that the marshes here have not kept up with an increase in the rate of sea-level rise during the last two decades.

1. Introduction

The relative elevation of the sediment surface within salt marsh landscapes is a critically important variable that determines the duration and frequency that these habitats are submerged by the tides, which ultimately controls the productivity of

*Corresponding author. Email: morris@biol.sc.edu

International Journal of Remote Sensing
ISSN 0143-1161 print/ISSN 1366-5901 online © 2005 Taylor & Francis
http://www.tandf.co.uk/journals
DOI: 10.1080/01431160500219018

the salt marsh plant community (Morris *et al.* 2002). The dominant salt marsh macrophytes are said to be foundation species (Pennings and Bertness 2001) because of their modification of the physical environment and the effect they have on community structure (Bruno and Bertness 2001). However, the success of the macrophytes in maintaining their environment depends on a number of factors, including the relative rate of sea-level rise (land subsidence plus the eustatic change in sea level), sediment supply and tide range (Stevenson *et al.* 1986, Reed 1995).

Salt marshes are known to have maintained an elevation in equilibrium with sea level for 4000 years by the accumulation of mineral sediment and organic matter (Redfield 1965, 1972). Intertidal salt marshes occupy a broad, flat expanse of landscape often referred to as the marsh platform at an elevation that approximates that of mean high water (MHW) (Krone 1985). The elevation of the platform relative to sea level determines total wetland area, inundation frequency and duration and wetland productivity. However, there are gradients in elevation within salt marshes. At the land-margin of marshes in the southeastern USA, the marsh macrophytes are limited in their vertical distribution by desiccation and salt stress, while at the seaward margin the plants are presumably limited by hypoxia (stress from oxygen deficiency) of the root systems arising from submergence by the tides (Mendelssohn and Morris 2000). The salt marsh proper and its macrophytes occupy only a small region of the entire intertidal zone and this habitat range differs regionally as a function of tidal range and other factors (McKee and Patrick 1988).

Despite the recognized importance of relative elevation to the function of salt marsh ecosystems, to the authors' knowledge there has never been a critical assessment of the distribution of relative elevations within a salt marsh landscape. This paper summarizes the results of a study that addresses this question. The boundaries of various salt marsh habitats were delineated using high spatial resolution imagery and an artificial neural network. The habitat boundaries subsequently were cross-referenced with LIDAR data and elevations within the boundaries were sampled and referenced against local tide data.

2. Methods

2.1 *Study site*

North Inlet estuary (figure 1) is located along the southeastern coast of the USA in South Carolina. It has been the site of multidisciplinary ecological research for over three decades and is one of the National Oceanographic & Atmospheric Administration's (NOAA) National Estuarine Research Reserves. North Inlet is a tidally dominated, bar-built, salt marsh estuary with a watershed area of about $75\,km^2$ and minimal surface fresh water input. Intertidal marshes within the boundaries of the Reserve consist of about $29\,km^2$ of marsh punctuated by 121 km of creeks. North Inlet experiences a regular semi-diurnal tidal pattern with a mean tidal range of approximately 1.4 m (Finley 1975). Maximum tidal amplitude near the ocean is 2.2 m. Due to its shallow character, North Inlet is flushed thoroughly by the tides, with approximately 50% of its water ebbing into the ocean twice per day. About $11.3 \times 10^6\,m^3$ of water floods the estuary on an average tide (Nummedal and Humphries 1978). Total net precipitation is 44 cm (precipitation minus evapotranspiration) or $33 \times 10^6\,m^3$ annually within the entire watershed (about 0.4% of the tidal exchange) (Morris 2000).

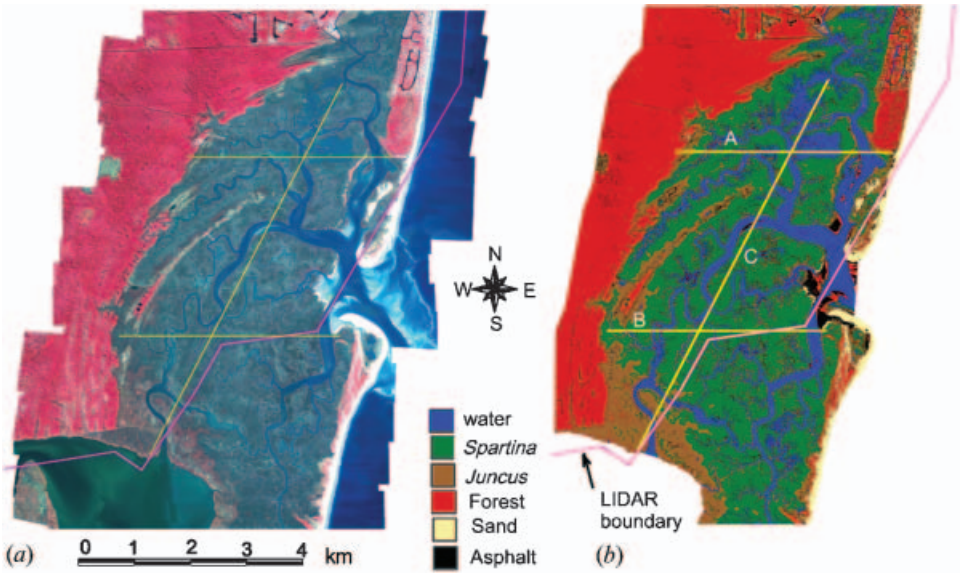

Figure 1. (*a*) A colour-infrared colour composite of the ADAR imagery of North Inlet in South Carolina obtained in 2000. (*b*) A land-cover classification map of North Inlet derived from the ADAR data. Transects crossing the marsh correspond to the cross-sections displayed in figure 3.

2.2 *Collection and processing of ADAR remote sensor data*

An ADAR 5500 digital camera system was used to acquire multi-spectral data in the following bandwidths: 450–515 nm (blue), 525–605 nm (green), 630–690 nm (red) and 750–860 nm (near-infrared). The data were obtained in October 2000 at an altitude of 2731 m above mean sea level, yielding a nominal spatial resolution of 0.7×0.7 m. The radiometric resolution was 8-bits per pixel. Remote sensor data acquisition was timed to coincide as near as possible with solar noon and low tide. This limited Sun angle effects and was the ideal time to undertake aerial photographic surveys of submersed habitat due to the elimination of tidal inundation effects (Jensen *et al*. 1998). Three flight lines of remote sensor data were recorded. Individual images had 35% endlap and sidelap and an average image footprint of 716×1075 m. Three types of radiometric non-uniformities were corrected by the data provider (Positive Systems, Inc.): (1) dark current noise, which is recorded by the charge-coupled device (CCD) regardless of whether or not incident energy (light) illuminated the detectors; (2) optical vignetting which causes imagery to appear darker toward the extreme edges of the field-of-view as compared to the centre; and (3) pixel-to-pixel non-uniformities (bright or dark pixels) caused by internal CCD sensor miscalibration.

Atmospheric correction of the ADAR data was performed using empirical line calibration (Jensen 2004). The spectral reflectance characteristics of a large, grey calibration target were measured *in situ* using a hand-held GER 1500 spectro-radiometer at the time of the overflight. The empirical line calibration forced the ADAR imagery to match the radiometric characteristics of the calibration target. This resulted in ADAR data measured in scaled surface spectral reflectance units. A limited number of ground control targets were located throughout the study area just prior to image acquisition. The X (easting), Y (northing) coordinates of the

panels were determined using a GPS Pathfinder® Pro XR Global Positioning System (GPS). The positional accuracy following post-processing was 50 cm with all coordinates stored in metres using the Universal Transverse Mercator (UTM) system (zone 17). The datum is the North American Datum (NAD) of 1983. The data collection vendor used the horizontal ground control information to geometrically rectify the ADAR 5500 individual scenes to a rms. error of 1 pixel (0.9 m).

2.3 *LIDAR data acquisition and processing*

The LIDAR data were collected by Airborne1, Inc., using an Optech ALTM 2025 sensor on January 16, 2003. At this time, the salt marsh vegetation in North Inlet was fully senesced. Airborne1, Inc. processed the data using vegetation removal algorithms to produce a bare-earth model with a 5 m nominal posting density. However, in open or unvegetated areas the nominal posting density was as high as 1.5 m. The LIDAR data, totalling approximately 45 million observations, were provided as text files containing X (easting), Y (northing), and Z (elevation) values in UTM 17 zone. Horizontal positions and elevation were based on NAD83 and NAVD88, respectively.

The text files were converted to ArcInfo coverages and then to a TIN (triangulated irregular network) using ESRI's ArcGIS 8.2 (Environmental Systems Research Institute) software. The *Createtin* function derives a TIN from a point, line or polygon coverage. This operation allowed points below a specified threshold to be deleted from the interpolation by setting the proximal tolerance. The proximal tolerance used in the creation of the TIN was 2.5 m. This allowed excess data points, between 2.5 m and the 5 m nominal posting density, to be excluded in the interpolation. In areas where no data points occurred within the desired 5 m posting, the TIN process interpolated from the nearest point. The resulting TIN has no data gaps, although the accuracy in some areas along the edges of the study area was degraded. The TIN was converted to a grid with a minimum mapping unit of 5×5 m using ArcGIS 8.2's TINLATTICE function.

2.4 *Artificial neural network training*

A back-propagation artificial neural network (NN) was used to extract land-cover habitat information from the ADAR imagery. The NN software was custom-designed using Java software and recommendations by Bishop (1995), Hagen *et al.* (1996), Reed and Marks (1999) and Principe *et al.* (2000) [see http://noble.ce.washington.edu (under Tools for data analysis) for a user interface and further details]. The NN architecture was optimized by adjusting the number of hidden neurons (1 to 8) and identifying the architecture that provided the best predictive model.

To train the NN, input data (ADAR reflectance values) and output data (numerical codes representing land-cover classes) were linearly scaled from 0.1 to 0.9. A logistic transfer function was used for hidden neurons, a linear transfer function was used for the output neuron (i.e. land classes) and a conjugate gradient error minimization was used to adjust the weights and biases during training. The model was trained and tested using 200 data points representing each cover class that were manually picked from the image. Ninety percent of the data were used for training and ten percent for testing.

2.5 *Vertical datums*

Tidal data (mean range, mean high water, mean high high water) from North Inlet were taken from a NOAA tide gauge situated within the estuary at Oyster Landing (station identification number 8662245; 33° 21.1′ N, 79° 11.2′ W). Monthly mean water levels from June 2001 to May 2003 were referenced to NAVD88 using the difference between mean low-low water (MLLW) and NAVD88 (NAVD88 – MLLW = 0.85 m) as referenced to the 1983–2001 epoch and as reported by NOAA for this site gauge.

A survey was conducted by the South Carolina Geodetic Survey (SCGS) during the spring of 2001 to establish ground control points in the salt marsh (Lapine 2001). Six sites were surveyed where stable benchmarks had been placed earlier (Childers *et al*. 1993). The survey was designed to meet the standards for first-order horizontal and 2 cm vertical accuracy. The survey used five Trimble 4000 SSi receivers, one Trimble 4700 receiver and one Trimble 4800 receiver. Each vector was observed twice for 1 hour each separated by either 21 or 24 hours. Sessions were scheduled to enable different satellite constellation configurations and a randomized weather pattern. Care was taken in planning and reconnaissance for the survey to ensure that the National Geodetic Survey (NGS) criteria for 2 cm ellipsoid height accuracy could be met. The horizontal control for the GPS project used three B-Order stations (GEORGETOWN 2, AERO and MULLET RM 3) and two first-order stations (4100 B and 4120 B). Additionally, two first-order benchmarks were included (U 147 and 866 2299 D TIDAL). Elevations were referenced to the SCGS datum cap installed on each benchmark. The first field observation period was conducted from 15 March 2001 to 17 March 2001. The second observation session was conducted from 3 May 2001 to 4 May 2001. Re-observations for two vectors took place on 8 May 2001.

3. Results

3.1 *Land-use classification*

Land classification was performed by applying a trained artificial neural network to the ADAR image. A logistic neural net model with five neurons in one hidden layer was used:

$$\begin{aligned} Y = {} & w_{1,1}/(1+\exp(-w_{1,2}X_1 - w_{1,3}X_2 - w_{1,4}X_3 - w_{1,5}X_4 - b_1)) + \\ & w_{2,1}/(1+\exp(-w_{2,2}X_1 - w_{2,3}X_2 - w_{2,4}X_3 - w_{2,5}X_4 - b_2)) + \ldots \\ & w_{5,1}/(1+\exp(-w_{5,2}X_1 - w_{5,3}X_2 - w_{5,4}X_3 - w_{5,5}X_4 - b_5)) + b_6 \end{aligned} \quad (1)$$

The output Y is a numerical value corresponding to the habitat class associated with the four reflectance values ($X_{i=1,4}$) of the ADAR blue, green, red and near-infrared bands. The model weights ($w_{i,j}$) and bias (b_i) values were determined by iterative training that gave the least sum of squares of the residuals of Y (table 1).

The output variable Y was an arbitrary numerical value between 0 and 1 chosen to represent water ($Y^*=0$), *S. alterniflora* marsh ($Y^*=0.2$), *Juncus* marsh ($Y^*=0.4$), forest ($Y^*=0.6$), asphalt ($Y^*=0.8$) or sand ($Y^*=1.0$). The input and output variables

Table 1. Weights ($w_{i,j}$) and bias (b_i) values used in the neural network model.

	$w_{i,1}$	$w_{i,2}$	$w_{i,3}$	$w_{i,4}$	$w_{i,5}$
$w_{1,j}$	−0.26735	7.621189	1.234	−6.271	−10.160
$w_{2,j}$	−3.95947	31.67067	21.818	18.311	−7.055
$w_{3,j}$	5.274324	7.485083	5.468	0.172	10.262
$w_{4,j}$	−4.28765	−44.2542	−19.837	−17.043	6.726
$w_{5,j}$	7.170576	−9.49441	−5.609	−1.721	−6.438
b_1	b_2	b_3	b_4	b_5	b_6
3.531	−16.108	−1.9016	17.8926	1.3382	−0.398

were scaled before the training procedure such that:

$$X = 0.1 + 0.8\left(X^* - X^*_{\min}\right)/X^*_{\max} \text{ and } Y = 0.1 + 0.8\left(Y^* - Y^*_{\min}\right)/X^*_{\min} \qquad (2)$$

where X^* and $Y^*$are the untransformed input and output variables, and $X^*_{\min}$, and $X^*_{\max}$ are the minimum and maximum values of X^* from the entire dataset (table 2) and $Y^*_{\min}$ and $Y^*_{\max}$ are the minimum and maximum outputs, or 0 and 1, respectively.

Results of the training procedure are shown in figure 2. There was little overlap between target values for water (0) and *S. alterniflora* habitat (0.2). The overlap could represent pixels of mixed class or misclassification by the neural network. Calculated target values of water (variable Y in equation (1)) among the $n=200$ training sample ranged from −0.81 to 0.202 with a mean of 0.003 ± 0.04. *S. alterniflora* pixels had calculated values ranging from 0.073 to 0.589 with a mean of 0.225 ± 0.073. Only 1.5% of classified water pixels fell within 2δ (two standard deviations) of *S. alterniflora* pixels, while 0.05% of classified *S. alterniflora* pixels fell within 2δ of classified water pixels. There was greater overlap between *Spartina* and *Juncus* (figure 2), although only 2% of classified *S. alterniflora* pixels fell within 2δ of *Juncus* and 2.5% of *Juncus* fell within 2δ of *Spartina*. Classified forest habitat had a mean calculated value of 0.593 ± 0.03 with a range of 0.48 to 0.67, and sand had a mean of 1.007 ± 0.02 ranging from 0.921 to 1.019. Only 0.5% of classified *Juncus* pixels fell within 2δ of classified forest, and 0% of classified forest fell within 2δ of *Juncus*. Thus, the delineation of *Juncus* and *Spartina* from other habitat types was excellent, while these two marsh types were distinguished from each other in about 90% of cases.

Percent cover of each marsh type and of water (subtidal habitat), computed over the entire image (figure 1), was consistent between images captured during 1999 (not shown) and 2000 (table 3). For example, the total area of marsh and water combined was estimated to be 41.8 km^2 during 1999 and 40.5 during 2000. One would expect trade-offs in subtidal and intertidal surface area, depending on the effects of sea-level rise or differences in tide level when the images were taken. However, the loss in

Table 2. Summary statistics of brightness values for blue, green, red and near-infrared (NIR) bands from the 2000 ADAR image of North Inlet.

	Blue	Green	Red	NIR
Maximum	232.0	255.0	255.0	255.0
Minimum	20.0	24.0	9.0	4.0
Mean	61.8	102.6	75.1	81.0
Range	212.0	231.0	246.0	251.0

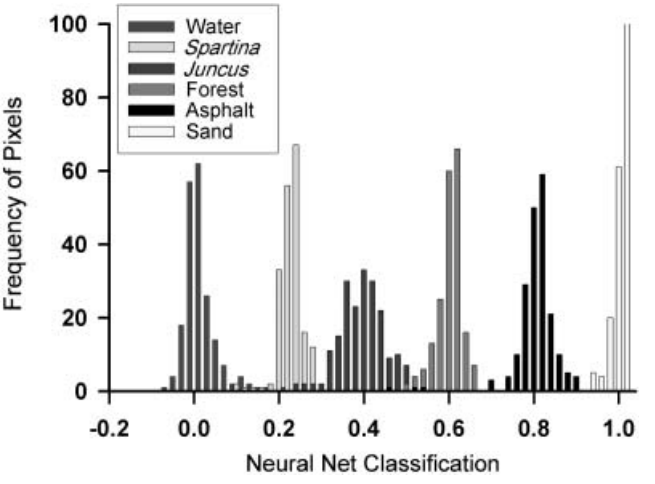

Figure 2. Frequency distributions of land cover obtained from the ADAR dataset used to train a five-neuron, one hidden layer artificial neural network. Each land-cover class consisted of reflectance values from 200 pixels collected from an ADAR image of North Inlet obtained in 2000 (see figure 1).

Juncus and *Spartina* habitat between 1999 and 2000, totalling 1.3 km^2, was greater than the gain in subtidal habitat (0.1 km^2, table 3), which suggests that there were gains in terrestrial habitat or tidal mud flats at the expense of tidal marsh habitat. However, the significance of these changes has not been evaluated and additional years of data are needed to establish a trend. Note that the area of water was quantified within boundaries drawn across the mouths of the inlets to the estuary (figure 1).

The subtidal area (permanently covered by water) of North Inlet is about 16% of the total estuarine area of 41 km^2 (table 3). The intertidal area is nearly evenly divided between *Juncus* and *S. alterniflora* habitats or about 83% of total estuarine area. Although the two marsh types are equivalent in area, their spatial distributions are quite different (figure 1). *Juncus roemerianus* marsh is found as a fringe around the upper edge of the *Spartina* marsh and as large monocultures in brackish regions of the estuary. Thus, the majority of habitat identified as *Juncus* lies along the border of Winyah Bay along the south side of North Inlet estuary.

3.2 *Marsh elevations*

LIDAR-derived marsh elevations compared favourably with the surveyed elevations (table 4). The difference between LIDAR and orthometric survey heights ranged

Table 3. Total areas by land-cover class (water, *Spartina alterniflora* marsh, *Juncus* marsh) in North Inlet, SC extracted from 1999 and 2000 ADAR images of the entire contiguous marsh and creek network including South Island.

Land-cover class	1999 area (km^2)	1999 area (% of total)	2000 area (km^2)	2000 area (% of total)
Water	6.6	15.8	6.7	16.6
S. alterniflora	18.3	43.8	17.5	43.2
Juncus	16.9	40.4	16.3	40.2
Total	41.8	100	40.5	100

Table 4. UTM coordinates, surveyed orthometric heights (m) and the corresponding LIDAR elevations (NAVD88) of sites within the salt marsh.

Site	*X* coordinate	*Y* coordinate	Orthometric heights (m)	
			Survey	LIDAR
Goat Island	667718.42876	3689498.13647	0.35	0.40
Bly Creek	667007.27245	3689128.92579	0.29	0.32
South Town Creek	666964.03053	3686943.93901	0.44	0.51
60 Bass Creek	668697.53911	3688847.58633	0.17	0.41
Debidue	670485.38925	3692704.34841	0.003	0.36
Old Man Creek	669887.25977	3691051.52020	0.26	0.35
Oyster	668381.06495	3691595.27473	0.13	0.23

from 5.5 cm to 35.6 cm. The mean difference of the six stations was 13 cm and the rms. error was 6.5 cm. Considering the low density of the 5×5 m LIDAR grid, the proximity of some benchmarks to nearby creeks, interference by vegetation, and waterlogged sediments, this degree of conformity is very good. In every case, the LIDAR-derived elevation was greater than the surveyed elevation, which suggests that a small bias exists in one of the datasets.

East–west transects across North Inlet generally slope downward from the east to the west (figure 3). Transect A, excluding the high ground on the east and west boundaries, has a negative slope of -5.8 cm km^{-1}. Transect B slopes -4.4 cm km^{-1} towards the west. Transect C, which runs from the south-west to the north-east, has a statistically significant ($p<0.0001$) slope of -0.85 cm km^{-1} (figure 3).

The *Spartina* marsh was classified at elevations almost entirely (99%) less than 0.6 m (LIDAR-derived elevations relative to NAVD88), or approximately below the elevation of MHW (0.618 m), and above MSL (figure 4). The *Spartina* marsh was 95% below 0.516 m, and the median elevation of the marsh was 0.349 m above NAVD88. The lower vertical boundary was about 0.104 m. Only 1% of the pixels classified as *Spartina* fell below that depth. The vertical range for 80% of the pixels classified as *Spartina* was 0.22 to 0.481 m.

The distributions of *Spartina* and *Juncus* were clearly different (figure 4). The *Juncus* marsh exhibited a broader vertical range than the *Spartina* marsh. Although there was some overlap in the classification of *Juncus* and *Spartina* and between *Juncus* and forest (see figure 2), one can predict that *Juncus* should have a greater range based on its growth habits, as discussed later. A few pixels classified as *Juncus* extended above 1.2 m in elevation and were probably misclassified. Ninety percent of the pixels classified as *Juncus* were less than 0.981 m in elevation, the median elevation was 0.519 m, and 1% were below 0.167 m.

The 'asphalt' class of land cover correctly identified a network of roads, but also was identified over a sandbar near the mouth of the inlet (figure 1). In the vicinity of the mouth there are exposed peat deposits that could be similar to asphalt in reflectance values, but the area classified as asphalt near the mouth is definitely not asphalt and is probably too great an area to be entirely peat.

4. Discussion

The slope of the landscape from east to west may be a consequence of barrier island migration landward. The origin of sediments may also influence the vertical

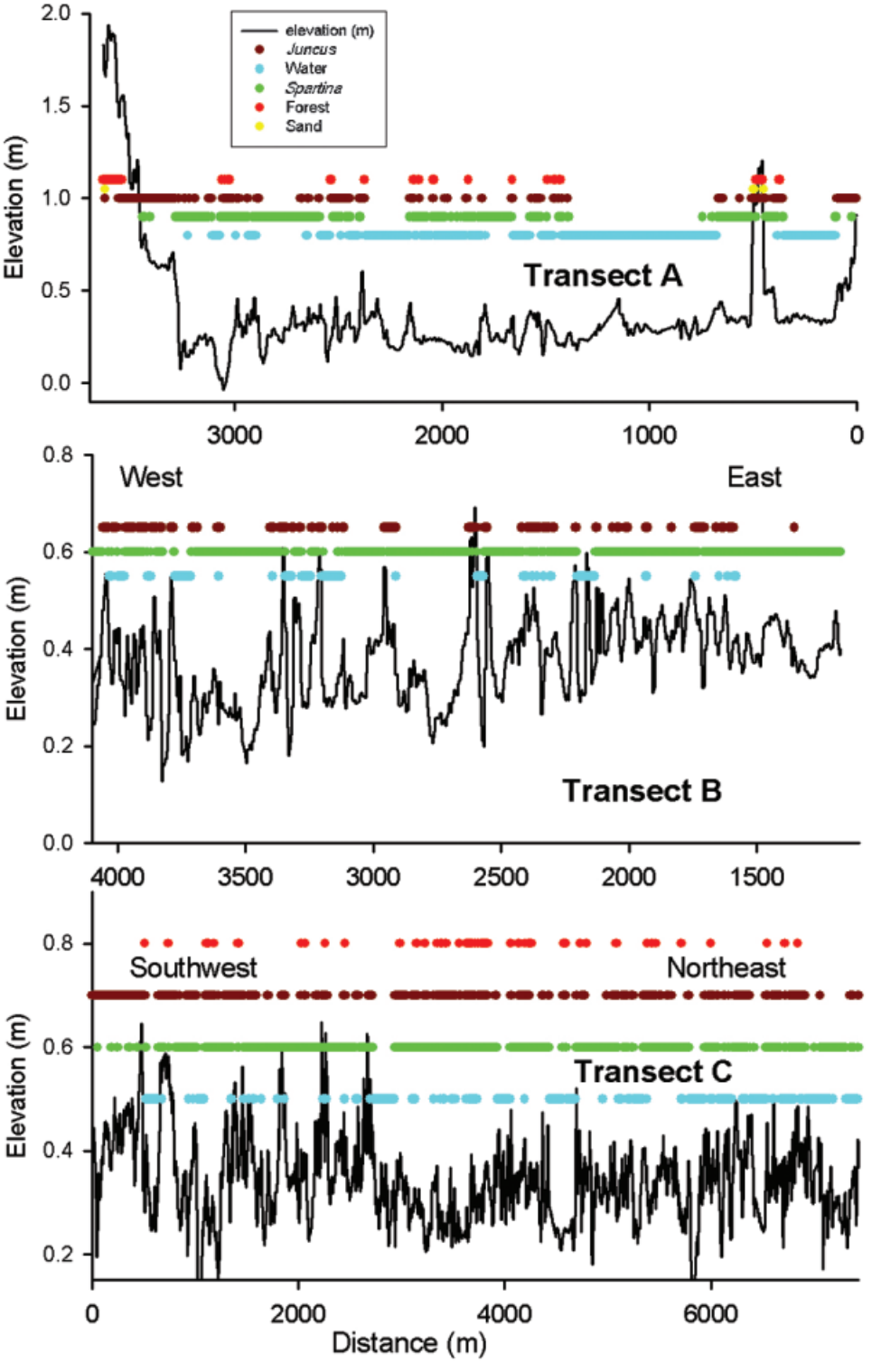

Figure 3. Elevations and land-cover habitat for transects A and B (see figure 1) across North Inlet trending east to west and C trending from the south-west to the north-east.

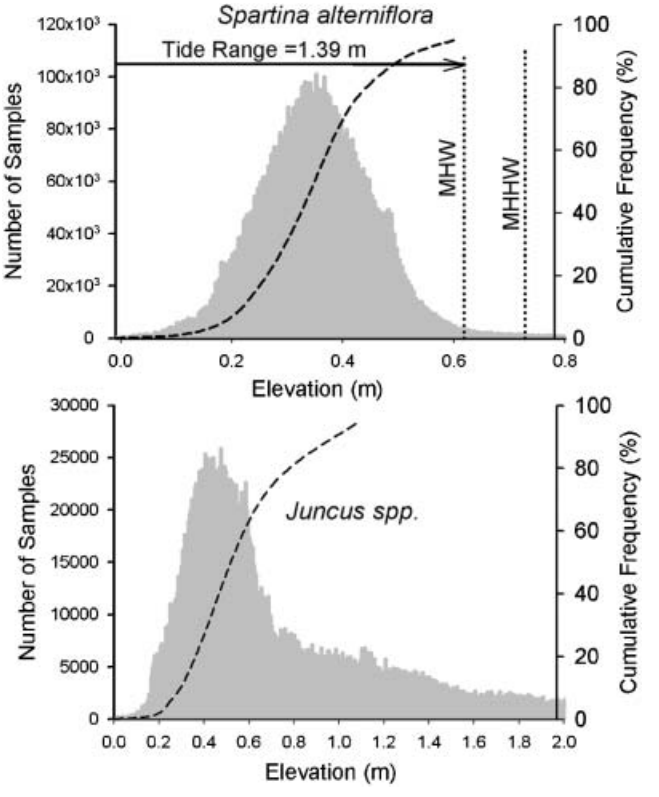

Figure 4. Frequency distributions (shaded area) and cumulative frequencies (dashed line) of elevations of pixels from a classified 2000 ADAR image of North Inlet. The ADAR image was classified using an artificial neural network and associated with elevations derived from LIDAR data. Elevations (m) are relative to NAVD88. Mean high water (MHW) and mean high high water (MHHW) were computed from monthly averaged water levels recorded at a NOAA tide gauge located at Oyster Landing (station 8662245) between June 2001 and May 2003.

gradients within the estuary (Gardner and Porter 2001). The major sediment source for North Inlet marshes is thought to be through the mouth of the inlet from the ocean. However, there appears to be a classical river berm (figure 3(*c*)) along the Winyah Bay side of North Inlet, which suggests that sediments from the Pee Dee River system enter North Inlet during flood events.

In the last two decades the primary productivity of North Inlet has increased, probably because the marsh surface has not kept pace with sea-level rise (Morris *et al*. 2002). This is supported by the analysis of marsh elevations that reveals that the majority of the marsh surface is 20 cm below MHW (figure 4). The equilibrium elevation of the marsh surface is inversely proportional to the rate of sea-level rise (Morris *et al*. 2002) and this also is consistent with the current distribution of marsh elevations.

Juncus apparently has a greater range of habitat in the vertical than *Spartina alterniflora*. The greater range of *Juncus roemerianus* is probably due to the presence of this species within the intertidal zone of the brackish region of the estuary as well as around the upper fringes of the salt marsh. The intertidal brackish regions

establish the lower vertical limit, and these brackish marshes are found on the south boarder of North Inlet on the Winyah Bay side of the estuary (see figure 1), while the upper vertical limits probably occur along the landward fringe of salt marshes.

The orthometric heights within the boundaries of *Spartina* habitat were normally distributed (figure 4). However, it has been argued that the tendency for salt marshes is to trap sediment until the elevation approaches that of MHW (Krone 1985), which should result in a distribution as shown in figure 5(*a*), with the marsh surface clustered at the high end of the range of *Spartina alterniflora*. *Spartina* traps sediments suspended in floodwater (Leonard and Luther 1995) and this process enables the marsh to maintain elevation in the face of rising sea level. However, Morris *et al.* (2002) have argued that the elevation of the marsh surface should be inversely related to the rate of sea-level rise. As the rate of sea-level rise increases, the median elevation should decrease and, because the edges of the marsh are not vertical, elevations across the marsh landscape should be normally distributed, as in figure 5(*b*). As rates of sea-level rise and/or land subsidence continue to increase, the equilibrium marsh elevation declines further, toward a lower limit where the duration of flooding is greater than the vegetation can tolerate. This results in a frequency distribution of marsh elevations that is focused around a lower limit, as in figure 5(*c*). Further, as the rate of sea-level rise increases and equilibrium marsh elevation declines, one would expect that the ratio of subtidal: intertidal area will increase as more of the lower edges of the marsh succumb to flooding and hypoxia. In other words, the area of open water within the estuarine landscape should increase. It is believed that these geomorphological metrics could be used to assess quickly the stability of coastal marsh landscapes.

The elevation of marsh relative to mean sea level and tidal range are important determinants of marsh primary productivity (Finley 1975). Soil salinity rises with increasing marsh elevation due to evapotranspiration (Morris 1995). Thus, maximum productivity per unit area occurs as sea level rises and equilibrium

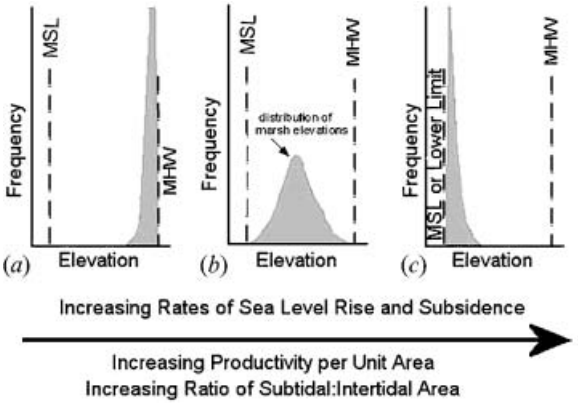

Figure 5. Hypothesized change in the frequency distribution of salt marsh elevations as a function of the rate of sea-level rise. The vertical distribution of the marsh is confined to a habitat range within the intertidal zone, and the distribution within that range is a function of the rates of sea-level rise, sediment accretion and land subsidence. Note that the mean elevation is in equilibrium with mean sea level and, therefore, the rate of sea-level rise relative to the marsh surface is zero in each example. It is thought that unit area productivity of the salt marsh and the ratio of subtidal: intertidal area also increase with rate of sea-level rise.

elevation declines (Morris *et al*. 2002). However, it is also argued that the total marsh area should decline with rising sea level, and the subtidal: intertidal ratio should increase, which suggests that the maximum marsh-wide, spatially integrated productivity should correspond to intermediate levels of sea-level rise, as appears to be the case at North Inlet. The interactions between the plants and their physical environment are reciprocal. The stresses on the marsh vegetation are determined in large part by the relative elevation of their habitat. These stresses determine primary productivity, which in turn affects sediment accretion and relative elevation.

5. Conclusions

A neural network was trained to classify high spatial resolution ADAR imagery of a salt marsh landscape at North Inlet, South Carolina, USA (see figures 1 and 2). Elevations of marsh habitats within North Inlet estuary were derived from LIDAR elevation data that were cross-referenced to the classified ADAR data and normalized to NAVD88. Mean absolute and rms. errors of LIDAR data were 0.133 m and 0.065 m, respectively, based on a comparison with seven orthometric survey heights scattered across the vegetated marsh and ranging in elevation from 0.003 m to 0.44 m (see table 4). The data suggest a positive bias in LIDAR elevation, probably as a consequence of interference from vegetation. The median LIDAR elevation of the salt marsh dominated by *Spartina alterniflora* was 0.35 m relative to NAVD88, or 0.43 m above the local mean sea level (based on June 2001 to May 2003 monthly data) and 0.27 m below the mean high water level.

The distribution of elevations of *Spartina* habitat within its vertical range was statistically normal, and 80% of the salt marsh was situated between a narrow range of 0.22 m and 0.481 m above NAVD88. In contrast, marsh area classified as being dominated by *Juncus roemerianus*, had a broader, skewed distribution with 80% of its distribution between 0.296 m and 0.981 m and a median elevation of 0.519 m (see figure 4). The intertidal marsh landscape was higher on the seaside than landside, suggesting landward migration of the barrier island, and higher on the Winyah Bay to the south, which suggests a sediment source from Winyah Bay (see figure 3). The relative elevation of the *Spartina* marsh at North Inlet is consistent with recent work that predicts a decrease in equilibrium elevation with an increasing rate of sea-level rise and suggests that the marshes here have not kept up with an increase in the rate of sea-level rise during the last two decades. It was suggested that the shape of the frequency distribution of salt marsh elevations is diagnostic of stability and that the elevations of marshes imminently threatened by rising relative sea level would be focused at the lower limit of elevation for the vegetation (see figure 5).

Acknowledgements

This research has been supported by a grant from the US Environmental Protection Agency's Science to Achieve Results (STAR) Estuarine and Great Lakes (EaGLe) program through funding to the ACE-INC, US EPA Agreement R82-867701. Although the research described in this article has been funded in part by the United States Environmental Protection Agency, it has not been subjected to the Agency's required peer and policy review and therefore does not necessarily reflect the views of the Agency and no official endorsement should be inferred. This research was also supported in part by the NSF LTREB and LTER programs, and NOAA. The authors thank several anonymous reviewers who provided helpful comments.

References

BISHOP, C.M., 1995, *Neural networks for pattern recognition* (Oxford, UK: Oxford University Press).

BRUNO, J.F. and BERTNESS, M.D., 2001, Habitat modification and facilitation in benthic marine communities. In *Marine Community Ecology*, M.D. Bertness, S.D. Gaines and M.E. Hay (Eds), pp. 201–218 (Sunderland, Massachusetts: Sinauer).

CHILDERS, D.L., SKLAR, F.H., DRAKE, B. and JORDAN, T., 1993, Seasonal measurements of sediment elevation in three mid-Atlantic estuaries. *Journal of Coastal Research*, **9**, pp. 986–1003.

FINLEY, R.J., 1975, Hydrodynamics and tidal deltas of North Inlet, South Carolina. In *Estuarine Research*, E. Cronin (Ed.), Vol. II, pp. 277–291 (NY: Academic Press).

GARDNER, L.R. and PORTER, D.E., 2001, Stratigraphy and geologic history of a southeastern salt marsh basin, North Inlet, South Carolina, USA. *Wetlands Ecology and Management*, **9**, pp. 371–385.

HAGEN, M.T., DEMUTH, H.B. and BEALE, M., 1996, *Neural network design* (NY: PWS Pub. Co).

JENSEN, J.R., 2004, *Introductory Digital Image Processing: A Remote Sensing Perspective*, 3rd edn (Upper Saddle River, NJ: Pearson Prentice Hall).

JENSEN, J.R., PORTER, D.E., COOMBS, C., JONES, B., WHITE, D. and SCHILL, S., 1998, Extraction of smooth cordgrass (*Spartina alterniflora*) biomass and leaf area index parameters from high resolution imagery. *Geocarto International*, **13**, pp. 25–34.

KRONE, R.B., 1985, Simulation of marsh growth under rising sea levels. In *Hydraulics and hydrology in the small computer age*, W.R. Waldrop (Ed.), pp. 106–115 (Reston, Virginia: Hydraulics Division, ASCE).

LAPINE, L.A., 2001, *Baruch Institute Tidal Studies, Georgetown, SC GPS Height Modernization 2001*, S.C. Geodetic Survey GPS Project Report (Columbia, SC).

LEONARD, L.A. and LUTHER, M.E., 1995, Flow dynamics in tidal marsh canopies. *Limnology and Oceanography*, **40**, pp. 1474–1484.

MCKEE, K.L. and PATRICK, W.H. JR., 1988, The relationship of smooth cordgrass (*Spartina alterniflora*) to tidal datums: a review. *Estuaries*, **11**, pp. 143–151.

MENDELSSOHN, I.A. and MORRIS, J.T., 2000, Ecophysiological controls on the growth of *Spartina alterniflora*. In *Concepts and Controversies in Tidal Marsh Ecology*, N.P. Weinstein and D.A. Kreeger (Eds), pp. 59–80 (Dordrecht: Kluwer Academic Publishers).

MORRIS, J.T., 1995, The salt and water balance of intertidal sediments: results from North Inlet, South Carolina. *Estuaries*, **18**, pp. 556–567.

MORRIS, J.T., 2000, Effects of sea level anomalies on estuarine processes. In *Estuarine Science: A Synthetic Approach to Research and Practice*, J. Hobbie (Ed.), pp. 107–127 (Washington D.C.: Island Press).

MORRIS, J.T., SUNDARESHWAR, P.V., NIETCH, C.T., KJERFVE, B. and CAHOON, D.R., 2002, Responses of coastal wetlands to rising sea level. *Ecology*, **83**, pp. 2869–2877.

NUMMEDAL, D. and HUMPHRIES, S.M., 1978, *Hydraulics and dynamics of North Inlet, South Carolina, 1975–76.* GITI Report 16 (Coastal Engineering Research Center, Fort Belvoir, VA: Department of the Army Corps of Engineers; and Vicksburg, MS: US Army Engineer Waterways Experiment Station).

PENNINGS, S.C. and BERTNESS, M.D., 2001, Salt marsh communities. In *Marine Community Ecology*, M.D. Bertness, S.D. Gaines and M.E. Hay (Eds), pp. 289–316 (Sunderland, Massachusetts: Sinauer).

PRINCIPE, J.C., EULIANO, N.R. and LEFEBVRE, W.C., 2000, *Neural and adaptive systems: fundamentals through simulations* (NY: Wiley and Sons).

REDFIELD, A.C., 1965, Ontogeny of a salt marsh estuary. *Science*, **147**, pp. 50–55.

REDFIELD, A.C., 1972, Development of a New England salt marsh. *Ecological Monographs*, **42**, pp. 201–237.

REED, D.J., 1995, The response of coastal marshes to sea-level rise: survival or submergence? *Earth Surface Processes and Landforms*, **20**, pp. 39–38.

REED, R.D. and MARKS, R.J., 1999, *Neural smithing: supervised learning in feedforward artificial neural networks* (Boston, MA: Massachusetts Institute of Technology).

STEVENSON, J.C., WARD, L.G. and KEARNEY, M.S., 1986, Vertical accretion in marshes with varying rates of sea-level rise. In *Estuarine Variability*, D.A. Wolfe (Ed.), pp. 241–259 (New York: Academic Press).